

Modeling of Hybrid Permanent Magnet - Gas Bearings

Stefano Morosi, smo@mek.dtu.dk

Ilmar F. Santos, ifs@mek.dtu.dk

Department of Mechanical Engineering, DTU - Technical University of Denmark, Nils Koppels Allé, 2800 Kgs. Lyngby, Denmark

Abstract. *Modern turbomachinery applications require nowadays ever-growing rotational speeds and high degree of reliability. It then becomes natural to focus the attention of the research to contact-free bearings elements. The present alternatives focus on gas lubricated journal bearings or magnetic bearings. In the present paper both the technologies are combined with the aim of developing a new kind of hybrid permanent magnetic - gas bearing. This new kind of machine is intended to exploit the benefits of the two technologies while minimizing their drawbacks. The poor start-up and low speed operation performance of the gas bearing is balanced by the properties of the passive magnetic one. At high speeds the dynamic characteristics of the gas bearing are improved by offsetting the stator ring of the permanent magnetic bearing. Furthermore this design shows a kind of redundancy, which offers soft failure properties. In the present paper, a detailed mathematical modeling of the gas bearing based on the compressible form of the Reynolds equation is presented. Perturbation theory is applied in order to identify the dynamic characteristic of the bearing. Due to the simple design of the magnetic bearings elements - being concentric rings with radial magnetic orientation - analytical expressions for the calculation of the magnetic flux density and forces are employed, opposed to the main literature trend where finite element software is utilized at least for the calculation of the B-field. Numerical analysis shows how the rotor equilibrium position can be made independent on the rotational speed and applied load; it becomes function of the passive magnetic bearing offset. By adjusting the offset it is possible to significantly influence the dynamic coefficients of the hybrid bearing.*

Keywords: Rotordynamics, Magnetism, Reynolds Equation, Fluid Film Bearings

1. INTRODUCTION

Gas lubrication represents a relatively recent development of fluid film bearing theory. Despite sharing a common base principle, for which a carrying load is developed as a result of viscous shear stress generation, the main difference is that compressibility effects need to be taken into consideration. Due to the fact that the lubricant, typically air, has a much lower viscosity than oil, gas bearings are characterized by lower carrying capacity, higher rotational speed and lower film thickness. This reduced clearance implies the need for a superior degree of surface finishing, to minimize the risk of contact between surfaces. Moreover, as the load capacity and dynamic properties are proportional to the operational speed, gas bearing are generally characterized by poor start-up and shut-down properties (Hamrock, 1994) (Constantinescu et al., 1985).

Recent progress in magnetic materials science has made feasible the application for passive magnetic bearing purposes. Active magnetic bearings have been used for several years, however they typically offer a modest force to weight ratio and require complex and expensive control systems and back-up system in case of controller or power failure (Kjølhed, 2007). As a consequence they have been often relegated to high performance mechatronic systems. Passive magnetic bearings are on the other hand simple, relatively cheap and light-weight. Their disadvantages are however a lower load capacity and poor dynamic properties (Mayer and Vesley, 2003).

The combination of the two technologies is characterized by several advantages:

- friction forces are very limited, close to zero, even at high rotational speed. As a consequence, heat generation is also very low. This is of great advantage for the magnetic bearing, which has an upper operational limit determined by the Curie temperature of the material;
- gas lubricants are generally very stable with respects to the temperature, they cannot boil, freeze or become flammable;
- contrary to oil lubricants, air viscosity increases with increasing temperatures, thus overheating provides additional carrying capacity.
- operation is possible at rotational speeds that exceed the maximum admissible for rolling or even oil lubricated journal bearings;
- there is no contamination of the surfaces, making them suitable for applications where a clean environment is required;
- contact free lubrication has low acoustic noise;
- the lack of carrying capacity at low speeds of the gas bearing is provided by the magnetic one;

- at higher speed, when the aerodynamic lift suffices to carry the load, the magnetic bearing can be used to improve the dynamic characteristics by offsetting the stator ring magnet.

This paper presents firstly a detailed analytical modeling of the two bearing alone and secondly a comparison with a combination of one gas and two magnetic bearings working in parallel. The main original contribution of the work is of theoretical nature. The bearings are part of a mechanical system comprised of a rigid rotor with two degrees of freedom, allowing translations in the horizontal and vertical directions.

The static and dynamic performance of a cylindrical hydrodynamic gas bearing is evaluated by the means of a perturbation analysis (Lund and Thomsen, 1978) (Santos et al., 2001) (SanAndres and Faria, 2000) (SanAndres and Kim, 2008), where expressions for the zeroth and first order field are obtained by a finite difference method.

Analytical expressions for calculating the magnetic flux density and forces are derived for the characterization of a magnetic bearing consisting of two concentric, radially magnetized rings (Baatz and Hyrenbach, 1991). A ferromagnetic jacket shielding is included in the design of the bearing with the purpose of enhancing the load carrying capacity (Mayer and Vesley, 2003). This coefficient is obtained by the means of a FE analysis software.

Numerical analysis is focused around typical operational parameters for the designed bearing; the load range is between 5-20 kg and the rotational speed of 10,000-30,000 rpm. The static analysis suggests that the hybrid bearing can operate independently from these parameters at constant eccentricity; this can be achieved by modifying the offset of the outer ring magnets using, for example, piezo-actuators. Adopting this strategy it is shown that it is possible to modify and enhance the dynamic coefficients of the bearing as function of the offset.

2. ANALYTICAL MODELING OF THE HYBRID BEARING

2.1 Gas Bearing

The pressure distribution p in a gas lubricated journal bearing is governed by the standard Reynolds equation:

$$\frac{\partial}{\partial y} \left(\rho \frac{h^3}{\mu} \frac{\partial p}{\partial y} \right) + \frac{\partial}{\partial z} \left(\rho \frac{h^3}{\mu} \frac{\partial p}{\partial z} \right) = 6U \frac{\partial \rho h}{\partial y} + 12 \frac{\partial(\rho h)}{\partial t} \quad (1)$$

where (y, z) are the circumferential and axial coordinates on the plane of the bearing. The viscosity μ can be considered as function of pressure and temperature. In gases this parameter is marginally affected by variations of pressure and; moreover is reasonable to assume that gas bearings work in near-isothermal conditions, as frictional heat generation is very low. Therefore μ is assumed to be constant (Hamrock, 1994). However the density is not constant, due to the compressibility property of gases. The ideal gas law states that:

$$\rho = \frac{p\tilde{M}}{RT} \quad (2)$$

where \tilde{M} is the molar mass of the gas, R is the universal gas constant and T the gas temperature. In isothermal conditions all these quantities are constant, thus introducing Eq. (2) into (1) yields:

$$\frac{\partial}{\partial y} \left(p h^3 \frac{\partial p}{\partial y} \right) + \frac{\partial}{\partial z} \left(p h^3 \frac{\partial p}{\partial z} \right) = 6\mu U \frac{\partial(ph)}{\partial y} + 12\mu \frac{\partial(ph)}{\partial t} \quad (3)$$

which is a nonlinear parabolic equation for the pressure. The boundary conditions for Eq. (3) are:

- the pressure at the bearing sides equals the atmospheric pressure p_{atm} :

$$p(y, 0) = p(y, b) = p_{atm} \quad (4)$$

- the pressure is continuous and periodic in the circumferential direction:

$$p(y, z) = p(y + 2\pi, z) \quad (5)$$

$$\frac{\partial p(y, z)}{\partial y} = \frac{\partial p(y + 2\pi, z)}{\partial y} \quad (6)$$

Film thickness. The location of the minimum film thickness is defined by the attitude angle Φ , see Fig. 1 and 2.

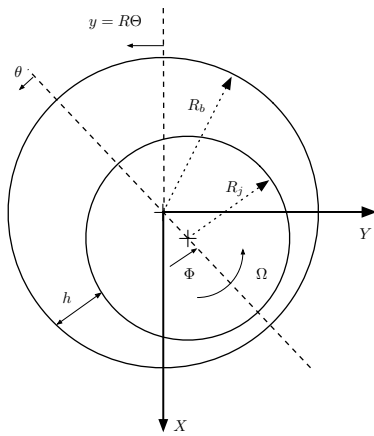


Figure 1. Journal bearing schematic.

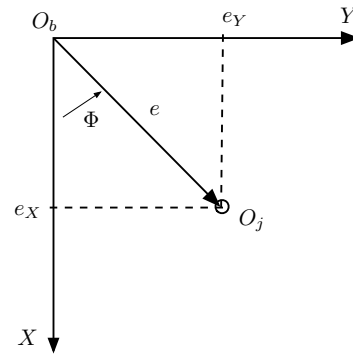


Figure 2. Definition of the journal eccentricity.

The circumferential coordinate is therefore redefined taking into account the attitude angle as:

$$y = \Theta R, \quad \Theta = \theta + \Phi \quad (7)$$

The journal center O_j is displaced a distance e from the bearing center O_b . This distance is known as the journal eccentricity and may vary with time depending upon the imposed external load on the bearing. The journal eccentricity cannot exceed the bearing clearance, to avoid solid contact between the surfaces. The eccentricity components in the inertial coordinate system are:

$$e_X = e \cos \Phi, \quad e_Y = e \sin \Phi \quad (8)$$

The film thickness function $h = h(y, t)$ depends on the position of the center of the shaft according to:

$$h = C + e_X \cos \Theta + e_Y \sin \Theta \quad (9)$$

where $C = R_b - R_j$ is the radial clearance of the bearing. [4]

Perturbation equations The general motion of the rotor at frequency (ω) with small amplitude harmonic motion $(\Delta e_X, \Delta e_Y)$ around an equilibrium position (e_{X_0}, e_{Y_0}) is:

$$e_X = e_{X_0} + \Delta e_X e^{i\omega t} \quad e_Y = e_{Y_0} + \Delta e_Y e^{i\omega t} \quad (10)$$

leading to the following perturbation expression for the film thickness function and pressure field:

$$h = C + e_{X_0} \cos \Theta + e_{Y_0} \sin \Theta + (\Delta e_X \cos \Theta + \Delta e_Y \sin \Theta) e^{i\omega t} \quad (11)$$

$$p = p_0 + (\Delta e_X p_X + \Delta e_Y p_Y) e^{i\omega t} \quad (12)$$

Separating steady state (zeroth order) and perturbed (first order) terms:

$$h = h_0 + \Delta h e^{i\omega t} \quad (13)$$

$$p = p_0 + \Delta p e^{i\omega t} \quad (14)$$

Equation (13) and (14) can be inserted into (3), yielding (neglecting higher order terms) the zeroth and first order lubrication equations:

- Zeroth order

$$\frac{\partial}{\partial y} \left(p_0 h_0^3 \frac{\partial p_0}{\partial y} \right) + \frac{\partial}{\partial z} \left(p_0 h_0^3 \frac{\partial p_0}{\partial z} \right) = 6\mu U \frac{\partial (p_0 h_0)}{\partial y} \quad (15)$$

- First order

$$\begin{aligned} X : \frac{\partial}{\partial y} \left(p_0 h_0^3 \frac{\partial p_X}{\partial y} + p_X h_0^3 \frac{\partial p_0}{\partial y} \right) + \frac{\partial}{\partial z} \left(p_0 h_0^3 \frac{\partial p_X}{\partial z} + p_X h_0^3 \frac{\partial p_0}{\partial z} \right) + 6\mu U \frac{\partial}{\partial y} (p_X h_0) + 12\mu i\omega (h_0 p_X) \\ = - \frac{\partial}{\partial y} \left(3p_0 h_0^2 \frac{\partial p_0}{\partial y} \cos \Theta \right) - \frac{\partial}{\partial z} \left(3p_0 h_0^2 \frac{\partial p_0}{\partial z} \cos \Theta \right) + 6\mu U \frac{\partial}{\partial y} (p_0 \cos \Theta) + 12\mu i\omega (p_0 \cos \Theta) \end{aligned} \quad (16)$$

$$\begin{aligned}
 Y : \frac{\partial}{\partial y} \left(p_0 h_0^3 \frac{\partial p_Y}{\partial y} + p_Y h_0^3 \frac{\partial p_0}{\partial y} \right) + \frac{\partial}{\partial z} \left(p_0 h_0^3 \frac{\partial p_Y}{\partial z} + p_Y h_0^3 \frac{\partial p_0}{\partial z} \right) + 6\mu U \frac{\partial}{\partial y} (p_Y h_0) + 12\mu i\omega (h_0 p_Y) \\
 = - \frac{\partial}{\partial y} \left(3p_0 h_0^2 \frac{\partial p_0}{\partial y} \sin \Theta \right) - \frac{\partial}{\partial z} \left(3p_0 h_0^2 \frac{\partial p_0}{\partial z} \sin \Theta \right) + 6\mu U \frac{\partial}{\partial y} (p_0 \sin \Theta) + 12\mu i\omega (p_0 \sin \Theta)
 \end{aligned} \quad (17)$$

Zeroth order equation. For given operation conditions $U = \Omega R_j$ and excentricity, the nonlinear PDE (15) is solved using a finite difference approximation on a discretized domain of dimension $m \times n$ in the y and z coordinate respectively. The resulting algebraic system is also nonlinear in p_0 , therefore the solution cannot be achieved directly. In the present case, an iterative solution strategy is developed splitting the pressure terms in the Reynolds equation, Eq. (15) as:

$$\left[\frac{\partial}{\partial y} \left(p_0^\alpha h^3 \frac{\partial}{\partial y} \right) \right] p_0^\beta + \left[\frac{\partial}{\partial z} \left(p_0^\alpha h^3 \frac{\partial}{\partial z} \right) \right] p_0^\beta = \left[6\mu U \frac{\partial}{\partial y} (h) \right] p_0^\beta \quad (18)$$

Starting from an initial guess for p_0^α , the problem becomes linear in p_0^β and thus can be solved directly for this variable, which then becomes the new guess for the next iteration. The solution strategy is then run until the difference between the solutions of two successive iterations is smaller than a set tolerance. This approach has been verified to be generally more stable and faster than a Newton-Raphson scheme. Once a solution is produced the zeroth order pressure field is integrated over the bearing surface, which in turn imposes vertical and horizontal lubrication reaction forces:

$$F_X^{gas} = \int_0^L \int_0^{2\pi} (p_0 - p_{atm}) \cos \Theta R d\Theta dz \quad (19)$$

$$F_Y^{gas} = \int_0^L \int_0^{2\pi} (p_0 - p_{atm}) \sin \Theta R d\Theta dz$$

First order equations. The solution of the first order perturbation Eq. (16) and (17) for the perturbed pressures (p_X, p_Y) is straightforward, as these are linear PDEs. Given a zeroth order field p_0 they are solved via a finite difference scheme and subsequently integrated over the bearing surface to determine the stiffness and damping coefficients:

$$K + i\omega D = \int_0^L \int_0^{2\pi} \begin{bmatrix} p_X \cos \Theta & p_X \sin \Theta \\ p_Y \cos \Theta & p_Y \sin \Theta \end{bmatrix} R d\Theta dz \quad (20)$$

It is important to notice that the dynamic coefficients are dependent on the excitation frequency and that the model assumes small amplitude of perturbations (Arghir et al., 2006) (Santos et al., 2001).

2.2 Magnetic Bearing

For the calculations of the magnetic flux density B and magnetic force F_m , a permanent magnetic bearing consisting of two radially magnetized rings is considered. The dimensions, the coordinate system arrangement and relationship between spontaneous magnetization and equivalent surface current density are shown in Fig. 3. Three coordinate systems are used for the analysis: the cylindrical system (r_m, α_m, z_m) , the cartesian moving system (x_m, y_m, z_m) attached to the outer ring and the cartesian stationary system (u_m, v_m, w_m) attached to the inner ring (Baatz and Hyrenbach, 1991).

Outer ring. The equivalent surface current density for the outer ring is defined as the cross product of magnetization vector M_o and a normalized vector perpendicular to the magnet's faces n_{\pm} :

$$S_{F_o} = -n_{\pm} \times M_o \quad (21)$$

where the magnetization is defined as:

$$M_o = M \begin{bmatrix} \cos \alpha_m \\ \sin \alpha_m \\ 0 \end{bmatrix} \quad (22)$$

with M being the spontaneous magnetization of the material. The magnetic flux density B_o can then be obtained through the Biot-Savart law:

$$B_o = \frac{\mu_0}{4\pi} \int \int_A \frac{S_{F_o} \times R_{P'P}}{\|R_{P'P}\|^3} dA \quad (23)$$

where the vector $R_{P'P}$ is the distance between a generic point P on the inner ring magnet and a source point P' on the outer ring magnet:

$$R_{P'P} = \begin{bmatrix} X_m - r_m \cos \alpha_m \\ -r_m \sin \alpha_m \\ Z_m - z_m \end{bmatrix} \quad (24)$$

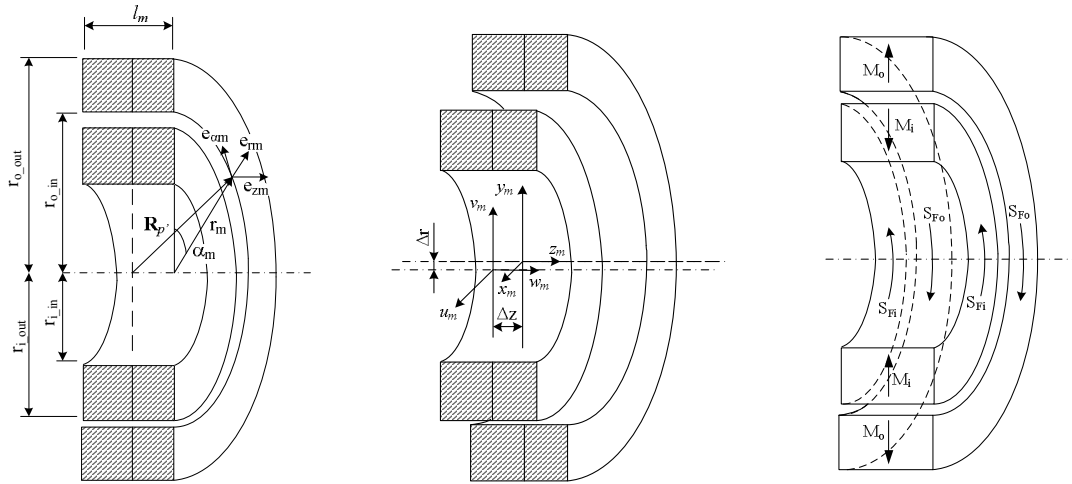


Figure 3. Characterization of the permanent magnetic bearing. From (Batz and Hyrenbach, 1991).

Inserting Eq. (21), (22) and (24) into (25), one obtains:

$$B_o = \frac{\mu_0}{4\pi} \int_{\alpha_m=0}^{2\pi} \int_{r_m=r_{o, in}}^{r_{o, out}} \frac{\begin{bmatrix} -\cos \alpha_m (Z_m - z_m) \\ -\sin \alpha_m (Z_m - z_m) \\ X_m \cos \alpha_m - r_m \end{bmatrix}}{[(X_m - r_m \cos \alpha_m)^2 + (r_m \sin \alpha_m)^2 + (Z_m - z_m)^2]^{3/2}} r_m dr_m d\alpha_m \quad (25)$$

$\left. \begin{array}{l} z_m = +l_a/2 \\ z_m = -l_a/2 \end{array} \right\}$

Inner ring. The spontaneous magnetization of the inner ring is equivalent to that of the outer one, see Eq. (22), however with opposite direction, see Fig. 3:

$$M_i = -M \begin{bmatrix} \cos \alpha_m \\ \sin \alpha_m \\ 0 \end{bmatrix} \quad (26)$$

With this quantity it is possible to calculate the equivalent surface current density on the inner ring:

$$S_{F_i} = -n_{\pm} \times M_i \quad (27)$$

Magnetic bearing force. The magnetic force between the two rings depends both on the magnetization of the inner ring, Eq. (26) and the magnetic field of the outer one, Eq. (25). If the surrounding of the bearing is filled with a material of unitary relative permeability, the force of a single current-carrying conductor within a magnetic field is given by:

$$F = \int_{\beta=0}^{2\pi} \int_{\rho_m=r_{i, in}}^{r_{i, out}} (S_{F_i} \times B_o) \rho_m d\rho_m d\beta_m \quad (28)$$

$\left. \begin{array}{l} w_m = +l_i/2 \\ w_m = -l_i/2 \end{array} \right\}$

In order to correctly describe the magnetic force for any point P of the moving reference of frame (x_m, y_m, z_m) in the fixed one, (u_m, v_m, w_m) , this should be rotated as show in Fig. 4. The distances X_m and Z_m are function of the position of ring magnets in relation to each other. Thus, these can be defined as:

$$X_m = \sqrt{(\Delta r_m + \rho_m \cos \beta)^2 + (\rho_m \sin \beta)^2} \quad (29)$$

$$Z_m = w_m + \Delta z_m$$

Note that if the rings are perfectly axially aligned, $Z_m = w_m$. The angle δ between the two coordinate systems is defined as:

$$\delta = \pm \frac{\rho_m \cos \beta + \Delta r_m}{X_m} \quad (30)$$

+ for $0 \leq \beta \leq \pi$ and - for $\pi \leq \beta \leq 2\pi$. The angle ϕ between X_m and ρ_m is also given as:

$$\phi = \begin{cases} \beta - \delta, & 0 \leq \beta \leq \pi \\ 2\pi - \beta + \delta, & \pi \leq \beta \leq 2\pi \end{cases} \quad (31)$$

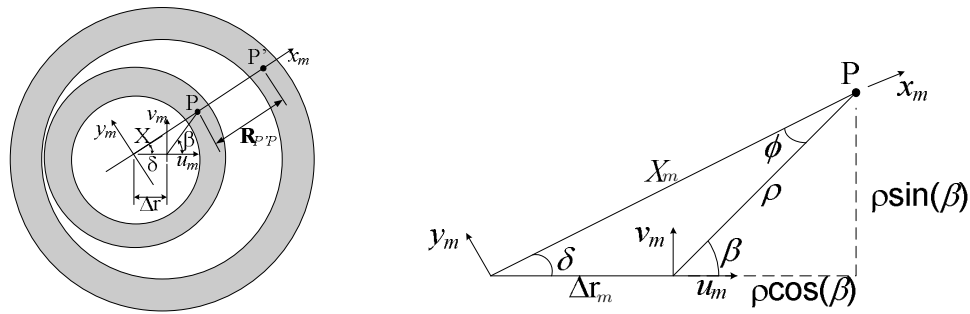


Figure 4. Magnetic bearing cross section, with displacement and coordinate system definition.

The magnetic flux density of the outer ring given in Eq. (25) is also rewritten in the fixed reference as:

$$B_o = \begin{bmatrix} B_{xi} \cos \delta \\ B_{xi} \sin \delta \\ B_{zi} \end{bmatrix} \quad (32)$$

It is finally possible to rewrite Eq. (28) as:

$$F = M_i \int_{\beta=0}^{2\pi} \int_{\rho_m=r_{in}}^{r_{out}} \begin{bmatrix} B_{zi} \cos \beta \\ B_{zi} \sin \beta \\ -B_{xi} \cos \phi \end{bmatrix} \Bigg|_{w_m=-l_i/2}^{w_m=+l_i/2} \rho_m d\rho_m d\beta \quad (33)$$

In order to increase the magnetic force, which in turns improves the load carrying capacity of the magnetic bearing, a possible strategy is to lower the reluctance of the paths of the magnetic flux outside the bearing, causing an increase of magnetic flux density in the air gap, see Fig. 5 and 6. This can be done quite easily by shielding the magnets with a soft ferromagnetic material of high permeability. The improvement of the characteristic curve (radial force vs. eccentricity) of the bearing is shown in Fig. 7. A shielding factor is calculated with the aid of the magnetic finite element software FEMM. Note that the slope of the characteristic curve is the stiffness of the bearing.

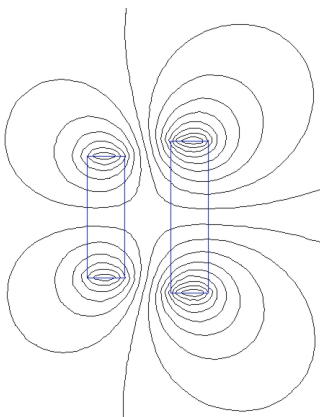


Figure 5. Magnetic flux density plot without shielding.

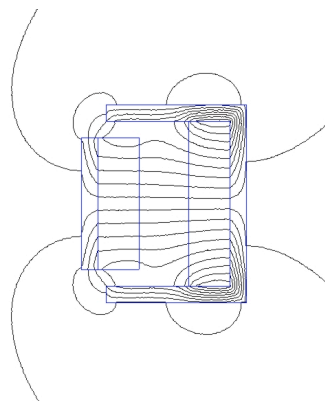


Figure 6. Magnetic flux density plot with shielding.

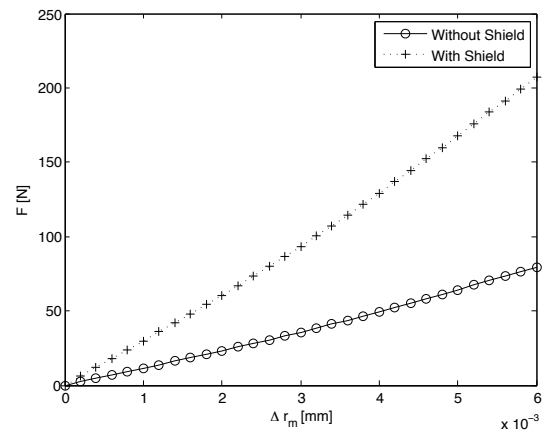


Figure 7. Characteristic curve of the magnetic bearing with and without shielding.

3. NUMERICAL ANALYSIS AND DISCUSSION

3.1 Steady state analysis

For a given position of the journal (e_X, e_Y), the Reynolds equation can be solved for the pressure, which in turn imposes vertical and horizontal lubrication forces on the shaft, see Eq. (19). Similarly, it is possible to calculate the magnetic forces on the shaft, as given in Eq. (33). Note that a further coordinate transformation is necessary in order to express the magnetic forces in the same reference as the gas ones. For a bearing to be in equilibrium the lubrication forces

must equilibrate a given load W acting on the vertical direction:

$$\begin{cases} W + F_X^{gas}(e_X, e_Y) + F_X^{mag-A}(e_X, e_Y) + F_X^{mag-B}(e_X, e_Y) = 0 \\ F_Y^{gas}(e_X, e_Y) + F_Y^{mag-A}(e_X, e_Y) + F_Y^{mag-B}(e_X, e_Y) = 0 \end{cases} \quad (34)$$

which is a nonlinear system that can be solved by a Newton-Raphson scheme with the Jacobian calculated via finite differences.

At this point it should be emphasized that the hybrid bearing is design to offer contact-free support in static conditions and during start-up or shut-down. However, the maximum relative eccentricity of the gas bearings is ca. 0.2% of the magnetic one, therefore the stator ring magnets should be vertically ($-X$ direction) offset in order to provide the carrying load at zero or low operational speed, see Fig. 8. The offset value can be found via another Newton-Raphson scheme analogous to the one presented in Eq. (34), however solved for the offset and not the equilibrium position. Note that the offset is a function of the required eccentricity, see Fig. 9. If the offset is kept constant as the rotational speed increases, the combination of magnetic and hydrodynamic forces tends to move the equilibrium position towards the center of the bearing. This is generally not preferable in hydrodynamic bearing operation. However, the problem is relatively easy to solve, as the required offset in order to keep a constant eccentricity can be calculated for any rotational speed and physically generated by piezo-actuators. With this strategy is then possible to define a priori a (constant) equilibrium position throughout a whole range of operational velocities and static loads, as opposed to a traditional hydrodynamic bearing, see Fig. 10 and 11.

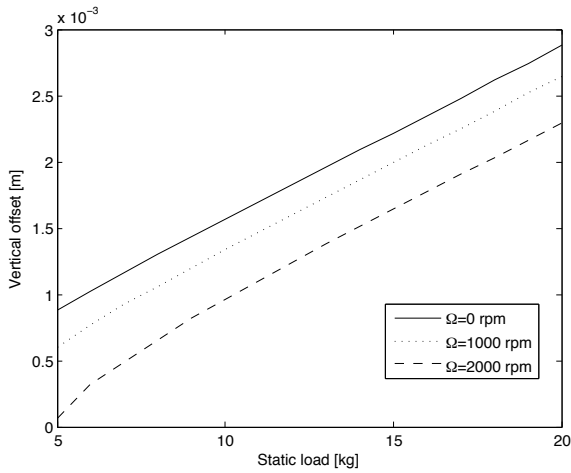


Figure 8. Required offset for keeping constant eccentricity $e = 0.75C$ as function of static load.

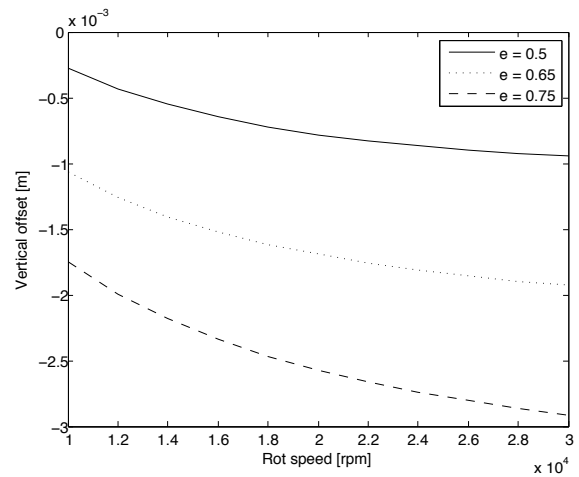


Figure 9. Required offset for keeping constant eccentricity e as function of the rotat. speed. ($W = 7$ kg).

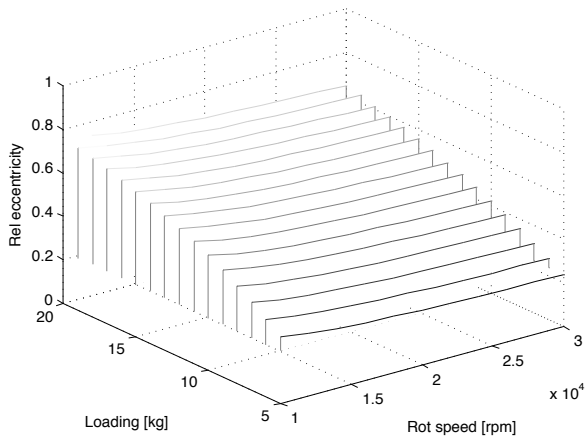


Figure 10. Relative eccentricity at equilibrium as function of rotational speed and load, gas bearing only.

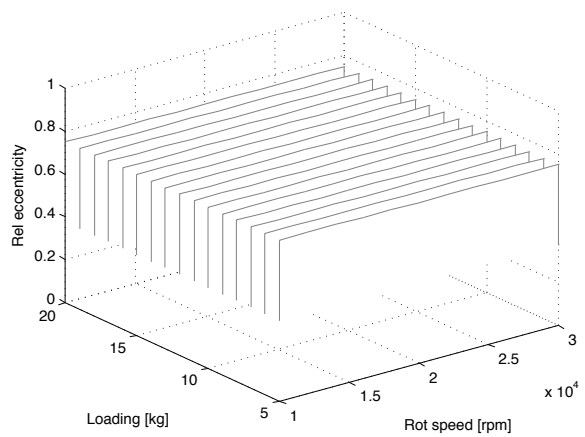


Figure 11. Relative eccentricity at equilibrium as function of rotational speed and load, hybrid bearing.

3.2 Dynamic analysis

The hybrid bearing is composed of one gas and two magnetic bearing in parallel; The physical representation of the dynamic coefficients and the schematic layout of the hybrid bearing is presented in Fig. 12 and 13.

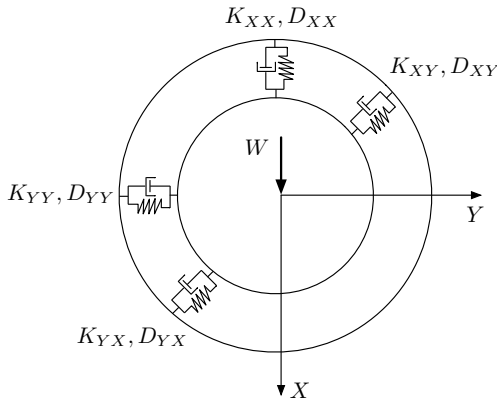


Figure 12. Physical representation of the dynamic coefficients of the bearing.

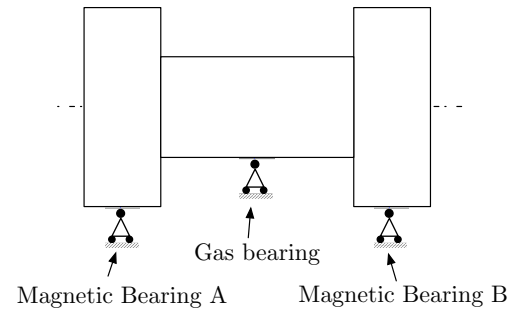


Figure 13. Schematic layout of the hybrid bearing.

The effective stiffness constant of the bearing is given by:

$$K = K^{gas} + K^{mag-A} + K^{mag-B} \quad (35)$$

However one should notice that the stiffness contribution of the magnetic bearing is around two orders of magnitude smaller than the gas bearing. As for the damping coefficient, it is assumed that the contribution of the passive magnetic bearing is negligible compared to the gas one:

$$D = D^{gas} \quad (36)$$

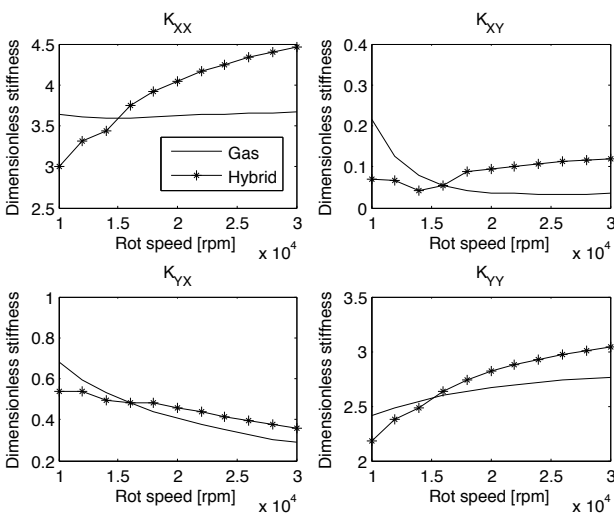


Figure 14. Stiffness coefficients as function of the rotational speed, gas bearing vs. hybrid bearing at $e=0.5C$.

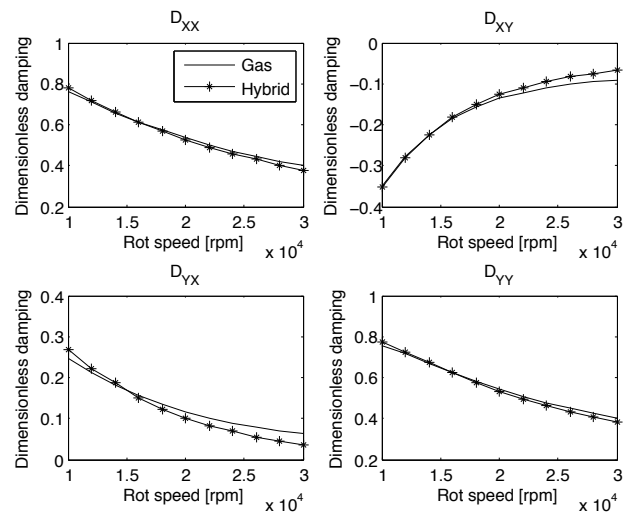


Figure 15. Damping coefficients as function of the rotational speed, gas bearing vs. hybrid bearing at $e=0.5C$.

The dynamic coefficients may be directly used in different rotor-dynamics calculations like unbalance response, random vibrations response, critical speeds and rotor stability (Lund and Orcutt, 1967) (Lund, 1968) (Lund, 1974) (Lund, 1976). In Fig. 14 to 17 a comparison between the synchronous dimensionless dynamic coefficients as function of the rotational speed of the gas bearing and hybrid bearing is presented. In both cases the simulations span at a typical operational range

of 10,000 - 30,000 rpm and with 10 kg of static load. Figure 14 and 15 are obtained imposing an eccentricity of $e=0.5C$ to the hybrid bearing. It is noticed that the stiffness coefficients are improved, although only after ca. 15,000 rpm; this behaviour relates to the eccentricity at which the gas bearing operates before and after this speed, as it will be explained subsequently. It is noticed that the damping coefficients cannot be considerably affected by the eccentricity (Arghir et al., 2006). This is confirmed by analyzing Fig. 17, which compares the damping coefficients of the gas bearing and the hybrid bearing at $e = 0.75C$. The direct coefficients in particular are only marginally altered, whereas the cross-coupled terms are characterized by larger deviations, sign inversions, although keeping the anti-symmetry typical of gas bearings (Czolczynski, 1996). On the other hand Fig. 16 clearly shows how operating at higher eccentricities the stiffness of the bearing considerably improves, with increments up to 200% for the direct coefficients, while maintaining overall symmetry of the cross-coupled terms.

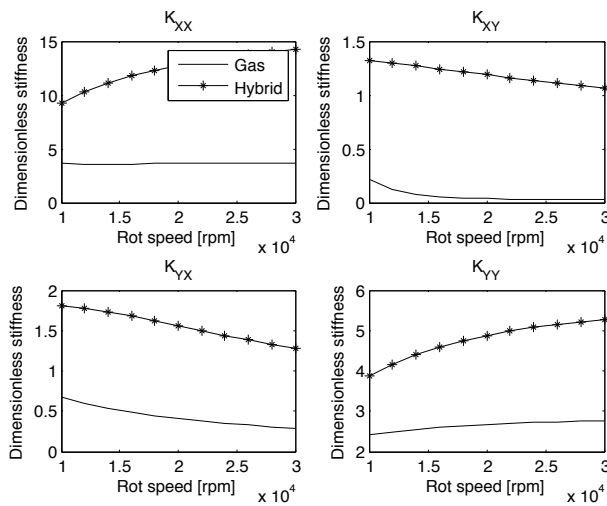


Figure 16. Stiffness coefficients as function of the rotational speed, gas bearing vs. hybrid bearing at $e=0.75C$.

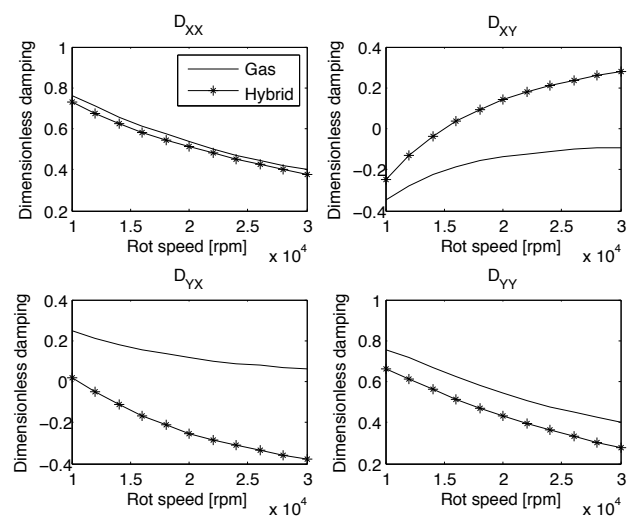


Figure 17. Damping coefficients as function of the rotational speed, gas bearing vs. hybrid bearing at $e=0.75C$.

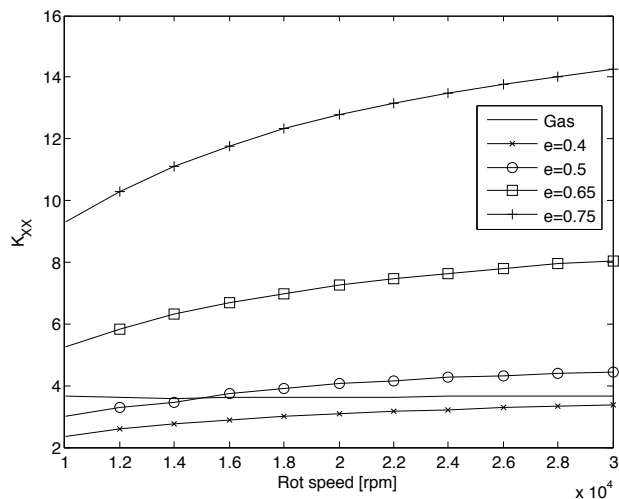


Figure 18. Vertical direct stiffness K_{XX} as function of the rotational speed.

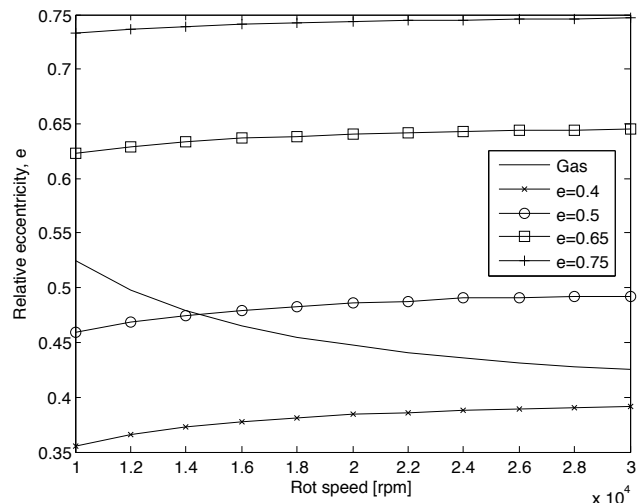


Figure 19. Relative eccentricity as function of the rotational speed.

The direct influence that imposing eccentricity has on the behaviour of bearing stiffness becomes clear analyzing Fig. 18 and 19, where the vertical direct stiffness coefficients K_{XX} and the relative eccentricity at equilibrium of the gas and hybrid bearing are presented as function of the rotational speed. Note that the load on the bearing is once again kept at a constant value of $W=10$ kg. It is interesting to notice that the value of the stiffness of the hybrid bearing is higher than

the one of the gas bearing only if the equilibrium position has higher eccentricity at the corresponding speed. Therefore, imposing an eccentricity $e = 0.4C$ to the hybrid bearing translates in lowering the value of K_{XX} compared to the gas bearing, throughout the whole velocity range. For $e = 0.5C$ the gas bearing has higher eccentricity up to ca. 15,000 rpm; thus, up to this threshold the gas bearing is stiffer. The maximum eccentricity of the gas bearing is about $0.53C$, meaning that for the cases of $e = 0.65C$ and $e = 0.75C$ the stiffness coefficients of the hybrid bearing are higher independently of the rotational speed.

4. CONCLUSION

This paper presents an analytical model for the calculations of the static and dynamic parameters of a hybrid permanent magnet - gas bearing. The combination of the two technologies improves the characteristic of the single elements; the limited carrying capacity of the self-acting gas bearing at low operational velocities can be provided by the magnetic bearing by carefully offsetting the stator ring magnets; when operating at higher speed the hydrodynamic forces are strong enough to carry the load and the passive magnetic bearing can be exploited in order to prescribe an operational eccentricity to the rotor by adjusting the offset. This in turns renders the equilibrium position of the bearing independent from the applied load and rotational speed. More importantly, having control over the eccentricity means that the dynamic coefficients can be modified and improved compared to a traditional gas bearing.

5. ACKNOWLEDGEMENTS

The authors would like to thank Lloyds Register ODS for the financial support of the project.

6. REFERENCES

- Arghir, M. et al., 2006, "Finite Volume Solution of the Compressible Reynolds Equation: Linear and Non-Linear Analysis of Gas Bearings", Proceedings IMechE Vol. 220, Part J: J. of Engineering Tribology.
- Baatz, M. and Hyrenbach, M., 1991, "Method of Calculating the Magnetic Flux Density and Forces in Contact-Free Magnetic Bearings", ETEP Vol. 1, No 4, 195-199.
- Constantinescu et Al., 1985, "Sliding Bearings", Allerton Press, translated from the Rumanian "Lagare cu Alunecare", 1980, Editura Technica.
- Czolczynsky, K., 1996, "How to Obtain Stiffness and Damping Coefficients of Gas Bearings", J. of Wear 201 (1996), 265-275.
- Hamrock, B.J., 1994, "Fundamentals in Fluid Film Lubrication", McGraw-Hill.
- Kjølhedde, K., 2007, "Experimental Contribution to the Problem of Model Identification in Rotating Machines via Active Magnetic Bearings", DCAMM Special Report No S101.
- Lund, J.W. and Orcutt, F.K., 1967, "Calculations and Experiments on the Unbalance Response of a Flexible Rotor", J. of Engineering for Industry, Trans. ASME, series B, Vol. 89, No 4, 785-796.
- Lund, J.W., 1968, "Calculation of Stiffness and Damping Properties of Gas Bearings", J. of Lubrication Technology, Trans. ASME, series F, 793-803.
- Lund, J.W., 1974, "Stability and Damped Critical Speeds of a Flexible Rotor in Fluid-Film Bearings", J. of Engineering for Industry, Trans. ASME, series B, Vol. 96, No 2, 509-517.
- Lund, J.W., 1976, "Linear Transient Response of a Flexible Rotor Supported in Gas-Lubricated Bearings", Journal of Lubrication Technology, Trans. ASME, Vol. 98, Series F, No 1, 57-65.
- Lund, J.W. and Thomsen, K.K., "Calculation Method and Data for the Dynamic Coefficients of Oil-Lubricated Journal Bearings", ASME Publication: Topics in Fluid Film Bearing and Rotor Bearing System Design and Optimization, pp. 1-28.
- Mayer, D. and Vesley, V., 2003, "Solution Of Contact-Free Passive Magnetic Bearing", J. of Electrical Engineering, Vol. 54, No 11-12, 293-297.
- San Andres, L. and Faria, M.T.C., 2000, "On the Numerical Modeling of High-Speed Hydrodynamic Gas Bearings", J. of Tribology, Trans. ASME, Vol. 122, 124-130.
- San Andres, L. and Kim, T. H., 2008, "Heavily Loaded Gas Foil Bearings: A Model Anchored to Test Data", J. of Engineering for Gas Turbines and Power, Vol. 130, 012504-1 - 012504-8.
- Santos, I.F. et Al., 2001, "Ein Beitrag Zur Aktiven Schmierungstheorie", Scwingungen in Rotierenden Maschinen, Vol 5, 21-30, in German.